

Electron and Ion Spectrometer (EIS) onboard the Nozomi spacecraft

A. Ihara¹, T. Doke², N. Hasebe², J. Kikuchi², M. -N. Kobayashi³, K. Maezawa¹, K. Nagata⁴, T. Sakaguchi⁵, T. Shino⁶, T. Takashima⁷, S. Teruhi⁸, B. Wilken⁹, and T. Yanagimachi¹⁰

¹Institute of Space and Astronautical Science, 3-1-1 Yoshinodai, Sagamihara, Kanagawa 229-8510, Japan

²Advanced Research Institute for Science and Engineering, Waseda University, 3-4-1 Okubo, Shinjuku-ku, Tokyo 169-8555, Japan

³Columbia Astrophysics Lab., Columbia University, Pupin Physics Lab., 550 West 120th Street, New York, NY, 10027, USA

⁴Faculty of Engineering, Tamagawa University, 6-1-1 Tamagawa Gakuen, Machida, Tokyo 194-8610, Japan

⁵Center for Nuclear Study, The University of Tokyo, 7-3-1 Hongo, Bunkyo-ku, Tokyo 113-0033, Japan

⁶Corporate Research and Development Center, Toshiba corp., 1 Komukaito-shibacho, Saiwai-ku, Kawasaki, Kanagawa 212-8582, Japan

⁷Department of Physics, Nagoya University, Furo-cho, Chikusa-ku, Nagoya, Aichi 464-8602, Japan

⁸Network Service Systems Lab., NTT corp., 1-1 Hikarinooka, Yokosuka-shi, Kanagawa 239-0847, Japan

⁹Max-Planck Institute for Aeronomy, Max-Planck Strasse, D-37191, Katlenburg-Lindau, Germany

¹⁰College of Science, Rikkyo University, 3-34-1 Nishi-ikebukuro, Toshima-ku, Tokyo 171-8501, Japan

Abstract. Nozomi was launched on July 4, 1998 as a Japanese first mission to the planet Mars. The main objective of this mission is to investigate the interaction between Martian atmosphere and the solar wind. The electron and ion spectrometer (EIS) is one of the fourteen instruments onboard the Nozomi spacecraft. EIS is designed to measure the fluxes of electrons, protons and heavy ions in the energy range from ~ 40 keV to a few MeV. It is a compact sensor of which the weight is 1.1 kg and the size is $80 \times 155 \times 207$ mm³. It consists of two kinds of telescopes based on the TOF \times E method (a TOF-E telescope) and on the $\Delta E \times E$ method (two ΔE -E telescopes). The ΔE -E telescopes are used to measure electrons and protons, while the TOF-E telescope is mainly used to measure He, CNO-group, NeMgSi-group, and Fe-group.

1 Introduction

Nozomi was launched on July 4, 1998 as a Japanese first mission to the planet Mars. The spacecraft was in a near-Earth orbit for the first five months. After that, it left the Earth for five years voyage toward Mars. The time of that insertion is planned to be between December 2003 and January 2004 (the orbit is shown in Fig. 1). During the cruise phase, some scientific instruments are working, and the others are switched off depending on their objectives. The full-scale observations by all instruments will be started at the same time as the deployment of antennas and booms after the spacecraft is inserted into an elliptical orbit around Mars.

The main objective of this mission is to investigate the interaction between Martian atmosphere and the solar wind. It was found by the observation with the Mars Global Surveyor

spacecraft that Mars has no intrinsic dipole magnetic field but has local magnetic fields whose sources are magnetized Martian crusts (Acuna *et al.*, 1999). From the standpoint of the shape of magnetic fields, Mars is different from Venus, non-magnetized planet, and, of course, from the Earth. Therefore, it cannot be predicted how the Martian atmosphere interacts with the solar wind. There are some observations related to this problem from several spacecraft. However, there are many questions unsolved about this interaction because the Martian magnetic field is more complicated than the dipole magnetic field of the Earth.

The electron and ion spectrometer (EIS) is one of the plasma detectors on the spacecraft. The main targets of the EIS measurements are to investigate (a) ion pick-up processes, (b) particle acceleration at the bow shock, (c) ion escape from Mars and (d) transport and energization of solar particles. To achieve this goal, we designed its observable energy range from ~ 40 keV to a few MeV. Although the main target of Nozomi is to investigate the physics of Mars, some scientific instruments are operated to do experiments during the cruise phase. EIS is one of them. We expect that EIS will contribute to the physics of interplanetary space; (e) Coronal Mass Ejections (CMEs) in interplanetary space and (f) particles from Corotating Interaction Region (CIR).

2 Sensor System

EIS is designed to measure the composition of electrons, protons and heavy ions in the energy range from ~ 40 keV to a few MeV. It is a compact sensor of which the weight is 1.1 kg and the size is $80 \times 155 \times 207$ mm³. It consists of two

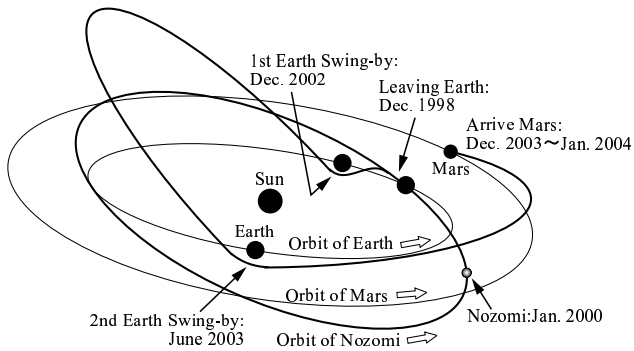


Fig. 1. Schematic drawing of EIS

kinds of telescopes based on TOF×E and $\Delta E \times E$ analyzing methods, respectively. Fig. 2 shows the schematic drawing of EIS. Four solid state detectors (SSDs: S1, S2, S3A and S3B) stacked in the case on the left side in Fig. 2 are all ion-implanted Si-detectors. S1 is used for the TOF-E telescope, S2 (E-detector) and S3A/S3B (ΔE -detector) for the ΔE -E telescopes. The TOF-E telescope looks in the 0° direction while the ΔE -E telescopes are oriented in the 180° direction. EIS is mounted on the spin-stabilized spacecraft (~8 sec/spin) looking perpendicular to the spin axis. Due to this configuration, these two kinds of telescopes cover the plane that is perpendicular to the spin axis of the spacecraft shown in Fig. 3. We describe EIS subsystems below.

2.1 TOF-E telescope

The TOF-E telescope employs the mirror-type TOF×E method. This method makes the spectrometer compact and enables it to satisfy the required conditions about size and weight. The field of view (FOV) of the TOF-E telescope is $\pm 8^\circ$. The telescope consists of a collimator made of aluminum, two microchannelplates (MCPs), one SSD (S1), a thin carbon foil, and an electrostatic reflector. The thin poly-carbonate front foil (about $10 \mu\text{g}/\text{cm}^2$), which is mounted on 78% transparency nickel grid, has a thin aluminum layer evaporated

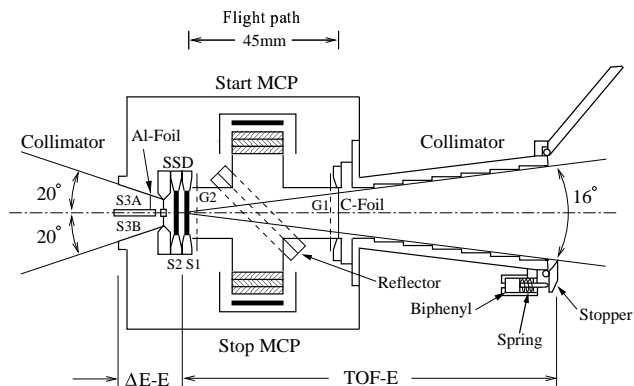


Fig. 2. Schematic drawing of EIS

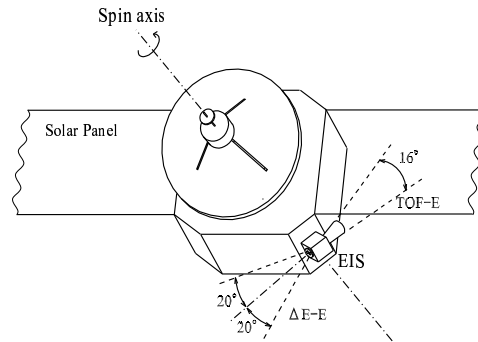


Fig. 3. Mounting of the EIS on the spacecraft

on its rear side in order to be stuck on the grid, and to prevent both sunlight and scattered background low energy particles from entering the telescope. As a result, its total thickness becomes $15.4 \mu\text{g}/\text{cm}^2$. The flight path of TOF, defined by the length between the foil and the Si-detector (S1) is 45 mm. The basic outline of the mirror-type TOF×E method is described in Reference (Wilken and Stüdemann, 1984).

Fig. 4 shows the schematic diagram of the electric potential distribution in the TOF-E telescope. When the incoming charged particle strikes the foil, secondary electrons are emitted from the thin foil. They are electrostatically accelerated to 600 eV, and their courses are deflected by 90° at the reflector which has an electrostatic field of $600 \text{ V}/0.3 \text{ cm} = 2000 \text{ V}/\text{cm}$. After that, they enter a MCP (14.5 mm in diameter) that generates an analog pulse to start the time measurement, while the incoming energetic ions pass through the reflector, being hardly affected by the electric field of $2000 \text{ V}/\text{cm}$. Finally when the particle hits the SSD and loses its energy, the SSD provides an E-signal whose pulse height is proportional to the lost energy. Simultaneously secondary electrons are emitted from the front surface of S1, and they are also accelerated by the grid G2 (600 V). After that, their flight path is also deflected by 90° at the reflector and they enter the other MCP, which provides the signal to stop the time measurement. Thus we obtain the particle velocity from the measured TOF and the flight path (45 mm). With the information of particle velocity (v) and energy (E), the mass (m) of the incoming particle can be determined by the equation $E = mv^2/2$.

The collimator has a baffled structure to reduce scattering of sunlight and electrons, and is covered by a cap to protect the thin carbon foil from a high level of sound emitted at launch. To open this cap when the spacecraft has entered a parking orbit around the Earth, the collimator is equipped with a small device having a spring and biphenyl that sublimates in a vacuum. The trick is that the biphenyl pressed by the spring begins to sublimate in a vacuum, and the wedge-shaped stopper that closes the cap moves bit by bit, toward the direction to finally open the cap by the gradually released pressure of that spring (right side of Fig. 2). It opens in ~24 hours (as expected from the ground base experiment) after

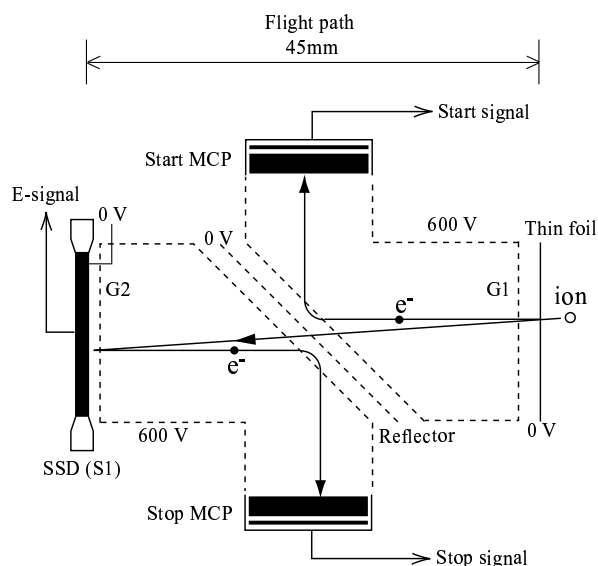


Fig. 4. Schematic diagram of the potential distribution in the spectrometer

the launch when the spacecraft is in a parking orbit around the Earth.

The TOF-E telescope measures protons in the energy range from 40 keV to 1.2 MeV, He from 60 keV to 1.7 MeV, CNO-group from 100 keV to 1.9 MeV, NeMgSi-group from 130 keV to 2.0 MeV and Fe-group from 260 keV to 2.3 MeV (shown in Table 1). The expected energy-flight time (E-T) relationship is shown in Fig. 5 (a). The TOF-E telescope has four energy thresholds, 27, 34, 40 and 62 keV, controlled by a command. The geometric factor of the TOF-E telescope is $0.015 \text{ cm}^2\text{sr}$ taking the shadow effect of the grid into account. In this TOF-E system, the time resolution is 1 nsec and the energy resolution is 29 keV, as calculated from the results of calibration pulses. The electric circuit noise for S1 or S2 equipped with a prototype pre-amplifier was 16 keV (FWHM) when tested on the ground.

Table 1. Target particles and its energy range of EIS

Particle	Energy (keV)		
	TOF-E	Si-A*	Si-B
electron	–	40–800	40–800
proton	40–1200	80–1700	40–1700
He	60–1700	–	–
CNO-group	100–1900	–	–
NeMgSi-group	130–2000	–	–
Fe-group	260–2300	–	–

* $154 \mu\text{g}/\text{cm}^2$ Al foil (40keV proton range in Al is $154 \mu\text{g}/\text{cm}^2$). ΔE -detector (S3A/S3B) is $\sim 9 \mu\text{m}=21 \text{ mg}/\text{cm}^2$, two E-detectors (S1 and S2) are $480 \mu\text{m}=1.1 \text{ g}/\text{cm}^2$.

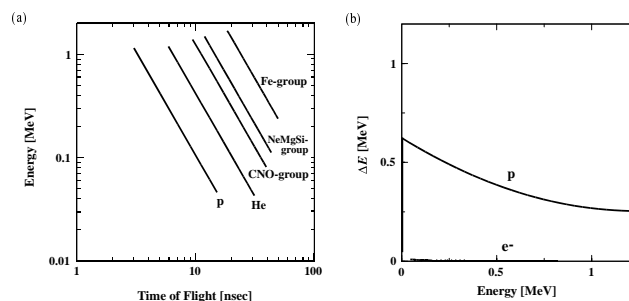


Fig. 5. Calculated responses of (a) the TOF-E telescope to various ions and (b) the ΔE -E telescopes to electrons and protons

2.2 ΔE -E telescopes

A schematic drawing of the ΔE -E telescopes is given on the left side of Fig. 2. The system of two identical telescopes is based on the well-known $\Delta\text{E}\times\text{E}$ method. These telescopes can measure electrons with energies from 40 to 800 keV, and protons from 40 keV to 1.7 MeV (Table 1). The expected ΔE -E curve calculated from the energy loss formulae (Ziegler *et al.*, 1985) is shown in Fig. 5 (b). Basically, the low energy threshold (40 keV) of the ΔE -E telescopes is determined by the detector noise. One of the telescopes (side-A) is covered with a thin aluminum foil, $154 \mu\text{g}/\text{cm}^2$ thickness, in order to prevent low energy ions ($<40 \text{ keV}$ for protons) from entering the telescope, and it permits the passage of electrons. In contrast, the other telescope (side-B) is not covered with a foil to pass low energy protons as well as electrons and high energetic protons. Low energy protons can be distinguished from electrons with the count-rate difference between side-A and side-B telescopes. The minimum detection energy for protons of the side-A ΔE -E telescope is $\sim 80 \text{ keV}$. These two telescopes have four discriminator levels for protons and electrons, respectively. These threshold levels are similar to that of TOF-E telescope. For the ΔE -E telescopes, the TOF-E Si-detector (S1) works as the anti-coincidence detector with a command.

Each ΔE -E telescope consists of two Si-detectors. One is a especially thin Si-detector (S3) of which the thickness is $8.8 \mu\text{m}$ for the side-A and $7.9 \mu\text{m}$ for the side-B, and the diameter is 4 mm. The other (S2) is almost the same as the S1 detector of the TOF-E telescope, of which the thickness is $480 \mu\text{m}$ and the diameter is 14 mm. The FOV of each ΔE -E telescope is 20° . An aluminum collimator located in front of the S3A/S3B detector defines the apertures of each telescope (its geometric factor is $0.027 \text{ cm}^2\text{sr}$).

We cannot acquire data from these two ΔE -E telescopes at the same time because S2 is used in common for both telescopes. Actually, only one of the two signals from S3A and S3B is effective in the digital part, and they are selected alternately every new sector i.e., every ~ 0.5 second (one spin is divided into 16 sectors in the EIS data handling system).

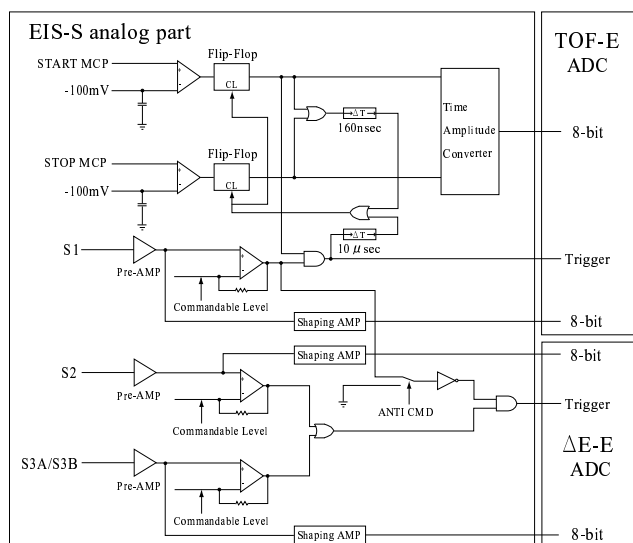


Fig. 6. Functional block diagram of the analog electronic system

3 Electronics

The electronic circuit of EIS consists of two parts, one of which is the analog part in the EIS sensor box (EIS-S) and the other is the digital part in the EIS electronics box (EIS-E). A functional block diagram of the analog part is shown in Fig. 6.

On the TOF-E part, the signals from two (START and STOP) MCPs are fed into the discriminators that create start and stop signals for the Time Amplitude Converter (TAC), respectively. If the stop signal is not produced within 160 nsec, the TAC judges that the event has no valid flight time information, and resets both START and STOP flip-flops. The range of TAC is set to be 80 nsec, and the event that gives the flight time between 80 nsec and 160 nsec will be recorded as a “saturated time event”. If the time interval between start and stop signals (= flight time) is within 80 nsec, the TAC produces a time signal (T-signal) whose pulse height is proportional to the flight time. After that, the signal is digitized by Analog Digital Converter (ADC) to form an 8-bit data. At the same moment, a charge signal from Si-detector (S1), whose pulse height is proportional to the energy deposited in S1 (E-signal), is amplified by the charge sensitive pre-amplifier (Pre-AMP). This E-signal is fed into the shaping-amplifier, and then 8-bit ADC converts the output signal to digital data as well. The E-signal from Pre-AMP is fed into the comparator, which is a command controllable discriminator, in order to check if the signal is valid or not. The comparator produces a signal which is used as the anti-coincidence signal for the $\Delta E-E$ analog part. Moreover, the coincidence signal between the Pre-AMP signal and the START MCP signal is used as a trigger for TOF-E data

acquisition.

On the $\Delta E-E$ part, the charge signals from the E-detector (S2) and the ΔE -detector (S3A/S3B) are fed into the corresponding Pre-AMPs and shaping amplifiers, and finally digitized by ADCs to be 8-bit data, respectively. Either signal from Pre-AMPs through the logical-OR is used as a trigger for $\Delta E-E$ data acquisition. This trigger logic enables the $\Delta E-E$ telescopes to obtain data of protons less than 670 keV that stop in the S3A/S3B. The anti-coincidence signal from TOF-E part can be used by a control command to reject particles that penetrates both S3A/S3B and S2. The functional digital part and the initial results of EIS are described in Reference (Ihara *et al.*, 2001).

The data packet of EIS consists of 432 bytes. The header, the first 24 bytes, provides command status, the frame counter, and housekeeping data, namely, the temperature of EIS-S or the voltage applied to MCPs. The remaining 408 bytes provide scientific data of both the TOF-E and $\Delta E-E$ telescopes. The header of a packet enables us to check if the scientific part of the packet is valid or invalid, and as a result, we can analyze the scientific data correctly.

4 Concluding remarks

In this paper, we describe the details of the EIS instrument. EIS is now monitoring solar energetic particles in interplanetary space. It has successfully observed several solar events like flares or CMEs. The particle data during the cruise phase will be used not only for the scientific purposes but also for check of our instrument. We can expect that EIS can achieve its mission purposes and contribute to science around Mars when Nozomi arrives at the planet in December 2003 or January 2004.

References

- Acuna, M. H., Connerney, J. E. P., Ness, N. F., Lin, R. P., Mitchell, D., Carlson, C. W., McFadden, J., Anderson, K. A., Rme, H., Mazelle, C., Vignes, D., Wasilewski, P., and Cloutier, P., *Global distribution of crustal magnetism discovered by the Mars Global Surveyor MAG/ER Experiment*, *Science*, 284, 790–793, 1999.
- Ihara, A., Doke, T., Hasebe, N., Kikuchi, J., Kobayashi, M. -N., Maezawa, K., Nagata, K., Sakaguchi, T., Shino, T., Takashima, T., Teruhi, S., Wilken, B., and Yanagimachi, T., *Electron and Ion Spectrometer (EIS) onboard the Nozomi spacecraft and its initial results in interplanetary space*, *Astroparticle Physics (submitted)*.
- Wilken, B. and Stüdemann, W., *A compact time-of-flight mass-spectrometer with electrostatic mirrors*, *Nucl. Instr. Meth. Phys. Res.*, 222, 587–600, 1984.
- Ziegler, J. F., Biersack, J. P., and Littmark, U., *The stopping and range of ions in solids*, Pergamon Press, 1985.